Published in final edited form as:
Nature. 2008 November 27; 456(7221): 502–506. doi:10.1038/nature07384.

Self-renewal and expansion of single transplanted muscle stem cells

Alessandra Sacco[1,*], **Regis Doyonnas**[1,*,†], **Peggy Kraft**[1], **Stefan Vitorovic**[1], and **Helen M. Blau**[1]

[1]Baxter Laboratory in Genetic Pharmacology, Department of Microbiology and Immunology, Stem Cell Institute, Stanford University School of Medicine, Stanford, California 94305-5175, USA.

Abstract

Adult muscle satellite cells have a principal role in postnatal skeletal muscle growth and regeneration1. Satellite cells reside as quiescent cells underneath the basal lamina that surrounds muscle fibres[2] and respond to damage by giving rise to transient amplifying cells (progenitors) and myoblasts that fuse with myofibres. Recent experiments showed that, in contrast to cultured myoblasts, satellite cells freshly isolated[3–5] or satellite cells derived from the transplantation of one intact myofibre6 contribute robustly to muscle repair. However, because satellite cells are known to be heterogeneous[4,6,7], clonal analysis is required to demonstrate stem cell function. Here we show that when a single luciferase-expressing muscle stem cell is transplanted into the muscle of mice it is capable of extensive proliferation, contributes to muscle fibres, and $Pax7^{+}luciferase^{+}$ mononucleated cells can be readily re-isolated, providing evidence of muscle stem cell self-renewal. In addition, we show using *in vivo* bioluminescence imaging that the dynamics of muscle stem cell behaviour during muscle repair can be followed in a manner not possible using traditional retrospective histological analyses. By imaging luciferase activity, real-time quantitative and kinetic analyses show that donor-derived muscle stem cells proliferate and engraft rapidly after injection until homeostasis is reached. On injury, donor-derived mononucleated cells generate massive waves of cell proliferation. Together, these results show that the progeny of a single luciferase-expressing muscle stem cell can both self-renew and differentiate after transplantation in mice, providing new evidence at the clonal level that self-renewal is an autonomous property of a single adult muscle stem cell.

We reasoned that prospective isolation of muscle stem cells (MuSCs) in conjunction with a dynamic analysis of their fate *in vivo* would greatly enhance our understanding of their potential to regenerate damaged muscle. Accordingly, we tested various fluorescence-activated cell sorting (FACS) fractionation procedures[3–5,7] and determined that, after depletion of CD45 (also known as Ptprc), CD11b (Itgam), Sca1 (Ly6a) and CD31 (Pecam1), a combination of endogenous markers—CD34 and integrin-α_7—enriched for a muscle cell population of morphologically round cells that uniformly expressed the satellite-cell-specific

Correspondence and requests for materials should be addressed to H.M.B. (hblau@stanford.edu).
†Present address: Pfizer Global Research & Development, Genetically Modified Models Center of Emphasis, Groton, Connecticut 06340, USA.
*These authors contributed equally to this work.

Supplementary Information is linked to the online version of the paper at www.nature.com/nature.

Author Contributions A.S., H.M.B. and R.D. designed the research, and A.S. and R.D. performed the experiments with support from P.K. S.V. performed single-cell RT–PCR. A.S. analysed the data. A.S., R.D. and H.M.B. discussed the results and wrote the paper.

transcription factor Pax7 (Fig. 1a–c). When isolated from *Myf5-nLacZ*^{Het} mice (in which the *nLacZ* reporter gene has been introduced into the locus of the myogenic transcription factor *Myf5* gene, expression of which is characteristic of activated satellite cells) and plated *in vitro*, these cells were activated (β-galactosidase$^+$ (β-gal$^+$); ref. [8] and Fig. 1d) and differentiated to form multinucleated myotubes (Fig. 1e). To determine the heterogeneity of this cell population, we performed single-cell reverse transcription followed by polymerase chain reaction for four transcripts for each of 40 FACS-isolated MuSCs (Fig. 1f and Supplementary Methods). Remarkably, all cells (100%) within this population expressed Pax7 andMyf5, characteristic of satellite cells9,10. Of these, 25% also expressed MyoD (also known as Myod1), a marker of committed progenitors11, and 12% expressed Pax3, a marker of progenitors intermediate between satellite cells and myoblasts in hindlimb muscles12,13. These data show that the CD34$^+$integrin-α_7^+ population is not fully homogeneous, because a subset of cells expressed commitment markers. To test the function of this muscle cell population *in vivo*, cells were transplanted into tibialis anterior muscles of non-obese diabetic/severely combined immuno-deficient (NOD/SCID) mice depleted of endogenous satellite cells by 18 Gy irradiation14,15. Four weeks after transplantation, muscles were damaged with notexin (NTX)16,17, and Myf5–β-gal$^+$ donor-derived cells were subsequently detected in the satellite cell position underneath the basal lamina of myofibres (Fig. 1g, h). This classical histological analysis demonstrated that this population of MuSCs homed to the satellite cell niche and responded appropriately to muscle damage by upregulating expression of the Myf5 transcription factor.

We reasoned that a dynamic assay could complement histological analyses by providing insights into the kinetics and extent of proliferation of transplanted MuSCs. We therefore developed a non-invasive bioluminescence imaging assay to monitor MuSCs by mating *Myf5-nLacZ*^{Het} mice with firefly luciferase (*FLuc*) transgenic mice[18]. In these studies, cell number was assessed as the bioluminescence signal derived from constitutive luciferase activity, and the activity of the *Myf5* promoter was assayed histologically as β-gal activity. The linearity, sensitivity and reproducibility of the bioluminescence assay for quantifying cell numbers was validated *in vitro* (Supplementary Fig. 1) and *in vivo* (Fig. 2a). The minimum number of cells detectable above control uninjected legs was 10,000 (Fig. 2a).

To validate bioluminescence imaging as an assay for MuSC function *in vivo*, we compared freshly isolated integrin-α_7^+CD34$^+$ MuSCs with cultured primary myoblasts, because previous studies by others indicated that these two cell types differ markedly[3]. We injected either 5,000 freshly isolated MuSCs or a fourfold excess of 20,000 cultured myoblasts[19–22], both isolated from the *Myf5-nLacZ/FLuc* transgenic mice, into irradiated legs of NOD/SCID recipients. Four weeks after transplantation, myoblasts were barely detectable ($0.2 \pm 0.01 \times 10^5$ photons cm^{-2} s^{-1}; Fig. 2b, top panels), indicating that their numbers had declined, whereas freshly isolated MuSCs yielded robust luciferase activity ($29.0 \pm 7.0 \times 10^5$ photons cm^{-2} s^{-1}), a signal corresponding to ~3×10^5 cells (Fig. 2b, top panels), which is approximately a 60-fold expansion (~6 doublings). Histological analysis revealed luciferase$^+$ myofibres in muscles of mice injected with freshly isolated MuSCs, but not myoblasts (Fig. 2b, middle panels). Histochemistry of NTX-damaged muscles revealed the presence of Myf5–β-gal$^+$ cells, indicative of activated satellite cells, after injection of uncultured MuSCs, but not myoblasts (Fig. 2b, bottom panels). Together, these results confirm that freshly isolated MuSCs, but not myoblasts, successfully engraft, proliferate and give rise to committed progenitors that contribute to muscle fibres.

To determine the proportion of cells with engraftment potential in this muscle cell population, we transplanted different numbers of freshly isolated MuSCs into irradiated tibialis anterior muscles. Bioluminescence was assayed four weeks after transplantation, and successful engraftment was defined as persistence of a signal >20,000 photons cm^{-2} s^{-1},

significantly above the background signal detected in control uninjected legs (Fig. 2c). More than 80% of mice showed engraftment when high numbers of MuSCs (500–5,000) were transplanted; however, even when as few as 10 cells were transplanted, 16% (2 out of 12 mice) showed engraftment (Fig. 2c). This percentage is probably the result of several hurdles such as the heterogeneity of the cell population (Fig. 1f), the survival rate of the cells after the isolation and injection procedures, and the threshold of detection by bioluminescence imaging. Notably, the signal plateaued in all cases (Fig. 2d), as reported for haematopoiesis[23], presumably reflecting a proliferation of cells until the need is met, after which a combination of cell death and quiescence leads to tissue homeostasis. The plateau occurred later and at a lower level when fewer cells were injected, suggesting that over time endogenous radiation-resistant satellite cells[15] increasingly compete with transplanted MuSCs for engraftment. In contrast with the marked increase in cell numbers that accompanies engraftment of freshly isolated MuSCs, cultured myoblasts decline in numbers within the first few days and then persist without detectable proliferation (Fig. 2e), consistent with previously published reports[24]. Furthermore, when MuSC-transplanted muscles with different engraftment levels were analysed, a linear correlation between the number of donor-derived myofibres and the bioluminescence signal was observed (Fig. 2f), further validating this dynamic assay as an ideal tool to quantify donor-derived cells *in vivo*.

A functional property of adult stem cells is the ability to repeatedly respond to tissue injury by giving rise to substantial numbers of proliferative progenitors. Accordingly, irradiated NOD/SCID mice were injected with 10 or 500 MuSCs (Fig. 3 and Supplementary Fig. 2). After engraftment, to evaluate the response of different numbers of MuSCs to injury, bioluminescence values for each mouse were normalized to the bioluminescence value obtained at the plateau of engraftment for that mouse. Mice were divided into two groups; one of these received NTX damage whereas the other did not. After NTX injury, transplanted cells underwent a second wave of ~80-fold expansion and, after a second injury with NTX, a third wave of ~100-fold expansion was observed, assessed as luciferase activity relative to the activity at the engraftment plateau. A peak was observed ~15 days post injury in each case (Fig. 3a, b and Supplementary Fig. 2), consistent with the timing of regeneration of 18-Gy-irradiated NOD/SCID muscles evident by morphology, by the presence of Myf5–β-gal$^+$ donor-derived cells and by the presence of regenerating myofibres expressing embryonic myosin heavy chain (Supplementary Fig. 3). This bioluminescence assay revealed a drop in cell number at the end of each regenerative wave of cell expansion, suggesting that cell death may counterbalance stem and progenitor cell proliferation to achieve homeostasis post injury. In contrast, luciferase activity in undamaged control mice remained relatively constant after engraftment (Fig. 3a and Supplementary Fig. 2). These results demonstrate that transplanted MuSCs can respond to serial injury with successive waves of progenitor expansion. The magnitude of the response to two sequential notexin injections suggests that stem cell function persisted over time.

To determine the basis for the accumulation of the bioluminescence signal in the course of regeneration, we analysed cell proliferation and apoptosis. Transverse sections of transplanted tibialis anterior muscles at days 7, 13 and 19 days post injury, revealed that donor-derived cells were proliferating as shown by the expression of the proliferative marker Ki67 in GFP$^+$ donor-derived cells (Supplementary Fig. 4). Thus, the ongoing proliferation over the three-week time period post injury supports the progressive accumulation of new donor-derived cells over time detected by bioluminescence. In contrast with proliferation, apoptosis slowly increased, and was highest at 19 days, suggesting that cell death could account for the decline in bioluminescence signal (Supplementary Fig. 5).

A potential caveat in these experiments is that the increase in luciferase signal might be due not only to changes in cell number but also to changes in the expression of the luciferase

gene or increased access of luciferin to luciferase$^+$ cells in a damaged tissue. To address these possibilities, muscles previously transplanted with myoblasts, as in Fig. 2e, were damaged by NTX injection. Instead of the bioluminescence signal increasing, it remained constant (Fig. 3a), indicating that luciferase activity is not affected by tissue damage and confirming that myoblasts are unable to achieve detectable proliferation in response to injury (Fig. 3a). Finally, we compared *in vitro* undifferentiated myoblasts and tibialis anterior myofibres isolated from *FLuc* transgenic mice and found that, per microgram of DNA, enzyme activity did not differ (Supplementary Fig. 6 and Supplementary Methods). These results demonstrate that luciferase activity constitutes a readout of muscle cell numbers.

To establish definitively that the MuSCs are capable of self-renewal *in vivo*, transplantation and analysis of the progeny of a single cell are required, the gold standard established for haematopoietic stem cells[23,25]. Because more than one cell (10–500 cells per muscle) was transplanted in the experiments described above, we could not rule out the possibility that different MuSCs gave rise to the three successive waves of progenitor proliferation (during engraftment and after two NTX injections) without ever giving rise to another muscle stem cell. To test this possibility, we performed single MuSC transplantation experiments (Fig. 4a and Supplementary Methods). In each of 2 independent experiments, 3 out of a total of 72 single cells (4%) exhibited engraftment above background levels four weeks after transplantation (Fig. 4b). These results revealed that the progeny of a single adult MuSC are capable of remarkable proliferation during engraftment, as in the six mice a signal approximately equivalent to 21,000–84,000 cells (~14–17 doublings) was detected. Notably, the bioluminescence assay enabled these single-cell studies, as detection of a 4% frequency using classical histological analyses would have been extremely labour-intensive. Histological analysis revealed that in those mice with a detectable bioluminescence signal, the progeny of a single cell differentiated and fused with mature myofibres (Fig. 4c). To determine whether self-renewal had occurred *in vivo*, we dissected the muscles and identified at least 50 donor-derived luciferase$^+$ cells per mouse expressing the satellite cell transcription factor Pax7 (81 ± 7% of total re-isolated luciferase$^+$ cells) two months after transplantation of a single cell (Fig. 4d). These results demonstrate that a single integrin-$\alpha_7{}^+$CD34$^+$ MuSC can self-renew, giving rise to a population of mononucleated Pax7$^+$ cells that stably reside in recipient muscles.

Here we provide evidence that adult MuSCs have self-renewal capacity *in vivo* by demonstrating that after transplantation a single cell is capable of both producing copies of itself and generating more specialized progenitors. Moreover, the bioluminescence imaging used in this report revealed the time course and unexpected magnitude of the proliferative response of which adult MuSCs and their progeny are capable *in vivo*, in contrast to myoblasts (Supplementary Fig. 7). This assay should have broad application for quantitative comparisons among cell types after delivery to solid tissues in diverse disease and injury models.

METHODS SUMMARY

Muscle stem cell isolation

Tibialis anterior muscles of mice were subjected to enzymatic dissociation (first collagenase 0.2% and then dispase (0.04 units ml^{-1}), Sigma) for 90 min, after which non-muscle tissue was gently removed under a dissection microscope. The cell suspension was filtered through a 70 μm nylon filter (Falcon) and incubated with the following biotinylated antibodies: CD45, CD11b, CD31 and Sca1 (BD Bioscience). Streptavidin beads (Miltenyi Biotech) were then added to the cells together with the following antibodies: integrin-α_7–phycoerythrin (PE; a gift from F. Rossi) and CD34–Alexa647 (eBioscience), after which

magnetic depletion of biotin-positive cells was performed. The ($CD45^-CD11b^-CD31^-Sca1^-$)$CD34^+$integrin-$\alpha_7^+$ population was then fractionated twice by flow cytometry (DIVA-Van, Becton-Dickinson). Primary myoblasts were isolated as described previously[20].

Bioluminescence imaging

For imaging, a Xenogen-100 device was used, as described previously[18]. In brief, the system comprises a light-tight imaging chamber, a charge-coupled device camera with a cryogenic refrigeration unit and the appropriate computer system (Living-Image Software; Xenogen). After intraperitoneal injection of luciferin in 100 μl of PBS (0.1 mmol per kg body weight, Xenogen), we acquired images continuously for 30 min and stored them for subsequent analysis. We analysed images at 15 min after luciferin injection.

Immunofluorescence and histology

Muscle tissues were prepared for histology as described previously17. For immunofluorescence, rabbit anti-β-galactosidase (Molecular Probes), rabbit anti-luciferase (Abcam), rabbit anti-GFP (Molecular Probes), rat anti-laminin (Upstate Technologies), mouse anti-Pax7 (Developmental Mouse Hybridoma Bank), mouse anti-myogenin (Pharmingen), rat anti-Ki67 (DAKO), mouse anti-embryonic-myosin-heavy-chain (F1.652)[26] and TUNEL (Apop TAG Red kit, Chemicon) were used.

Statistical analysis

Data are presented as mean ± s.e.m. Comparisons between groups used the Student's *t*-test assuming two-tailed distributions, with an alpha level of 0.01–0.05.

Supplementary Material

Refer to Web version on PubMed Central for supplementary material.

Acknowledgments

We thank O. Alkan for developing the single cell RT–PCR protocol, K. Koleckar, M. Pajcini and T. Doyle for technical support, T. Brazelton, F. Rossi and S. Corbel for comments on the manuscript, J. Ramunas for statistical analysis, and M. Lutolf and P. Gilbert for fabricating the hydrogel microwells. We also thank F. Rossi for providing the integrin-α_7–PE-conjugated antibody, and C. Contag for providing the *FLuc* mice. This work was supported by NIH grants AG009521, AG024987 and by the Baxter Foundation.

References

1. Charge SB, Rudnicki MA. Cellular and molecular regulation of muscle regeneration. Physiol. Rev 2004;84:209–238. [PubMed: 14715915]
2. Mauro A. Satellite cells of skeletal muscle fibers. J. Biophys. Biochem. Cytol 1961;9:493–495. [PubMed: 13768451]
3. Montarras D, et al. Direct isolation of satellite cells for skeletal muscle regeneration. Science 2005;309:2064–2067. [PubMed: 16141372]
4. Kuang S, et al. Asymmetric self-renewal and commitment of satellite stem cells in muscle. Cell 2007;129:999–1010. [PubMed: 17540178]
5. Cerletti M, et al. Highly efficient, functional engraftment of skeletal muscle stem cells in dystrophic muscles. Cell 2008;134:37–47. [PubMed: 18614009]
6. Collins CA, et al. Stem cell function, self-renewal, and behavioral heterogeneity of cells from the adult muscle satellite cell niche. Cell 2005;122:289–301. [PubMed: 16051152]
7. Sherwood RI, et al. Isolation of adult mouse myogenic precursors: functional heterogeneity of cells within and engrafting skeletal muscle. Cell 2004;119:543–554. [PubMed: 15537543]

8. Tajbakhsh S, et al. Gene targeting the *myf*-5 locus with *nlacZ* reveals expression of this myogenic factor in mature skeletal muscle fibers as well as early embryonic muscle. Dev. Dyn 1996;206:291–300. [PubMed: 8896984]
9. Seale P, et al. Pax7 is required for the specification of myogenic satellite cells. Cell 2000;102:777–786. [PubMed: 11030621]
10. Zammit PS, et al. Kinetics of myoblast proliferation show that resident satellite cells are competent to fully regenerate skeletal muscle fibers. Exp. Cell Res 2002;281:39–49. [PubMed: 12441128]
11. Zammit PS, et al. Muscle satellite cells adopt divergent fates: a mechanism for self-renewal? J. Cell Biol 2004;166:347–357. [PubMed: 15277541]
12. Conboy IM, Rando TA. The regulation of Notch signaling controls satellite cell activation and cell fate determination in postnatal myogenesis. Dev. Cell 2002;3:397–409. [PubMed: 12361602]
13. Boutet SC, et al. Regulation of Pax3 by proteasomal degradation of monoubiquitinated protein in skeletal muscle progenitors. Cell 2007;130:349–362. [PubMed: 17662948]
14. Wakeford S, Watt DJ, Partridge TA. X-irradiation improves mdx mouse muscle as a model of myofiber loss in DMD. Muscle Nerve 1991;14:42–50. [PubMed: 1992296]
15. Heslop L, Morgan JE, Partridge TA. Evidence for a myogenic stem cell that is exhausted in dystrophic muscle. J. Cell Sci 2000;113:2299–2308. [PubMed: 10825301]
16. Harris JB, Johnson MA. Further observations on the pathological responses of rat skeletal muscle to toxins isolated from the venom of the Australian tiger snake, *Notechis scutatus scutatus*. Clin. Exp. Pharmacol. Physiol 1978;5:587–600. [PubMed: 152684]
17. Sacco A, et al. IGF-I increases bone marrow contribution to adult skeletal muscle and enhances the fusion of myelomonocytic precursors. J. Cell Biol 2005;171:483–492. [PubMed: 16275752]
18. Wehrman TS, et al. Luminescent imaging of β-galactosidase activity in living subjects using sequential reporter-enzyme luminescence. Nature Methods 2006;3:295–301. [PubMed: 16554835]
19. Blau HM, Hughes SM. Retroviral lineage markers for assessing myoblast fate *in vivo*. Adv. Exp. Med. Biol 1990;280:201–203. [PubMed: 2123371]
20. Rando TA, Blau HM. Primary mouse myoblast purification, characterization, and transplantation for cell-mediated gene therapy. J. Cell Biol 1994;125:1275–1287. [PubMed: 8207057]
21. Rando TA, Pavlath GK, Blau HM. The fate of myoblasts following transplantation into mature muscle. Exp. Cell Res 1995;220:383–389. [PubMed: 7556447]
22. Gussoni E, Blau HM, Kunkel LM. The fate of individual myoblasts after transplantation into muscles of DMD patients. Nature Med 1997;3:970–977. [PubMed: 9288722]
23. Cao YA, et al. Shifting foci of hematopoiesis during reconstitution from single stem cells. Proc. Natl Acad. Sci. USA 2004;101:221–226. [PubMed: 14688412]
24. Barberi T, et al. Derivation of engraftable skeletal myoblasts from human embryonic stem cells. Nature Med 2007;13:642–648. [PubMed: 17417652]
25. Osawa M, et al. Long-term lymphohematopoietic reconstitution by a single CD34-low/negative hematopoietic stem cell. Science 1996;273:242–245. [PubMed: 8662508]
26. Silberstein L, et al. Developmental progression of myosin gene expression in cultured muscle cells. Cell 1986;46:1075–1081. [PubMed: 3530499]

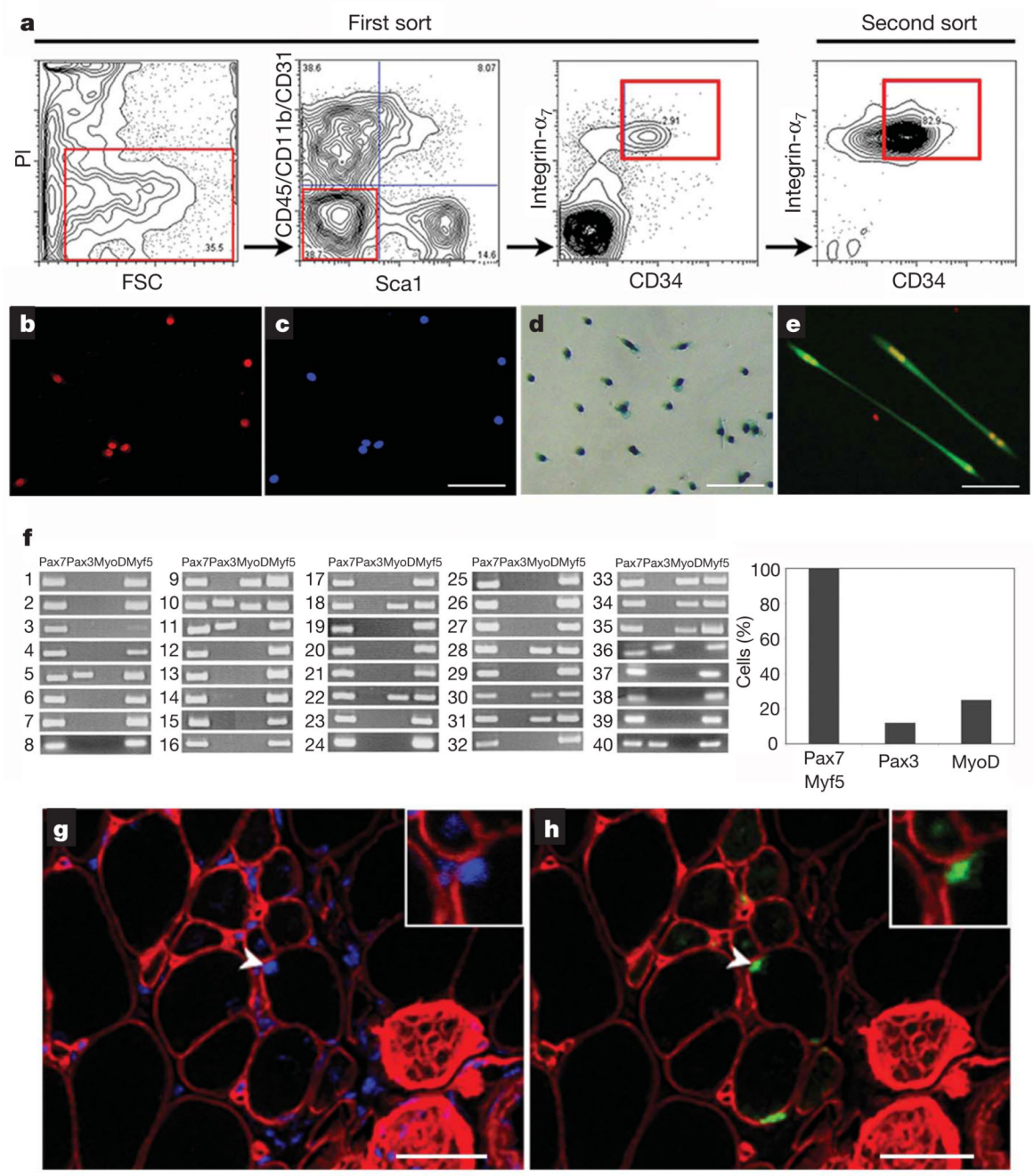

Figure 1. Characterization of the integrin-α_7^+CD34$^+$ fraction as muscle stem cells

a, Flow cytometry analysis of freshly isolated muscle cells. Living cells were gated for forward scatter (FSC) and propidium iodide (PI) negativity (left panel). Cells negative for blood markers CD45 and CD11b, for endothelial marker CD31 and for mesenchymal marker Sca1 were gated (middle-left panel), and within this population the integrin-α_7^+CD34$^+$ fraction was sorted (right panels). **b**, **c**, Forty-eight hours after isolation, muscle integrin-α_7^+CD34$^+$ cells were stained for Pax7 (left: Pax7, red; right: nuclei, blue). Scale bar, 80 μm. **d**, After 5 days of culture in growth medium, integrin-α_7^+CD34$^+$ cells isolated from *Myf5-nLacZ*^{Het} mice showed β-gal activity. Scale bar, 80 μm. **e**, After 3 days of culture in differentiation medium, integrin-α_7^+CD34$^+$ cells (from *GFP*-transgenic mice)

differentiated to form myotubes (green) that expressed myogenin (red). Scale bar, 80 μm. **f**, Single MuSCs (1–40) were individually sorted and reverse transcription followed by polymerase chain reaction performed as described in Supplementary Methods. The results show that this population consistently and homogeneously expresses Pax7 and Myf5, the expected transcriptional profile for satellite cells[8–10]. In contrast, both MyoD and Pax3 expression are heterogeneous, indicating the presence of committed progenitors, in accordance with previously published reports[11–13]. **g**, **h**, Freshly isolated integrin-α_7^+CD34$^+$ cells from *Myf5-nLacZ*^{Het} mice were transplanted into recipient mice. One month after transplant, recipient muscles were damaged by NTX injection and 5 days later immunofluorescence of transverse tissue sections revealed Myf5–β-gal$^+$ cells engrafted in the satellite cell position (arrowhead and inset). β-gal, green; laminin, red; nuclei, blue. Scale bars, 20 μm.

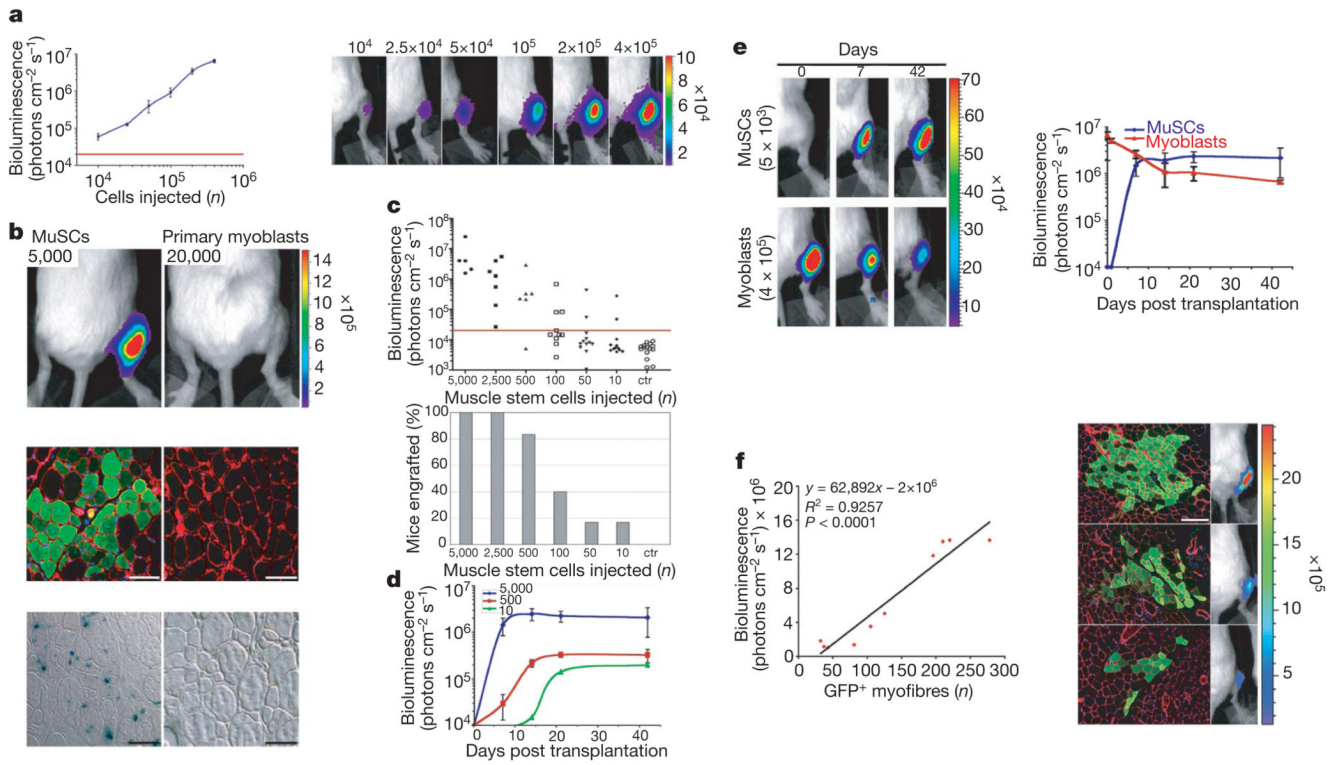

Figure 2. MuSC engraftment monitored by *in vivo* non-invasive bioluminescence imaging

a, Increasing numbers of myoblasts isolated from *Myf5-nLacZ/FLuc* mice were injected into the tibialis anterior muscles of NOD/SCID recipients and imaged 2 h after injection. Shown is a graph of bioluminescence data represented as average ± s.e.m. ($n = 4$; $P \leq 0.05$; left) and a bioluminescent image of representative injected mice, with the number of cells injected indicated at the top (bioluminescence values are indicated as photons cm^{-2} s^{-1} × 10^4; right). **b**, Top, freshly isolated MuSCs or cultured myoblasts from double-transgenic mice were injected into recipients and imaged four weeks after transplantation ($n = 4$; $P < 0.005$; bioluminescence values are indicated as photons cm^{-2} s^{-1} × 10^5). Middle panels, immunofluorescence of luciferase expression in transverse muscle sections reveal the contribution of MuSCs, not of myoblasts, to muscle fibres. Laminin, red; luciferase, green; nuclei, blue. Scale bars, 100 μm. Bottom, 5 days before tissue harvesting, muscles were damaged with NTX. β-gal staining revealed Myf5–β-gal^+ cells in muscles transplanted with MuSCs, not with myoblasts. Scale bars, 100 μm. **c**, Different numbers of MuSCs were injected into muscles of recipients ($n = 50$), and engraftment was measured by imaging four weeks after transplantation (uninjected legs are shown as negative control, ctr). A scattered graph of bioluminescent values of individual mice (top) and a histogram graph showing the percentages of mice with successful engraftment for each number of cells injected are shown (bottom). **d**, Engraftment of MuSCs (5,000, 500, 10) was monitored by imaging over a period of six weeks after transplantation (average ± s.e.m.; $n = 3$; $P < 0.05$). **e**, Freshly isolated MuSCs or cultured myoblasts were transplanted into recipients and engraftment was monitored by imaging over a period of six weeks after transplantation. Bioluminescent images of representative injected mice acquired at the indicated days are shown (bioluminescence values are indicated as photons cm^{-2} s^{-1} × 10^4; left). Graph of bioluminescence measurements (average ± s.e.m., $n = 5$; $P < 0.05$, right). **f**, MuSCs from *GFP/FLuc* transgenic mice were transplanted into recipients. Four weeks later, mice were analysed by bioluminescence imaging and for histology. Regression analysis shows a significant ($n = 10$, $P < 0.0001$) correlation between the number of GFP^+ myofibres and

luciferase activity in individual mice (left). Representative images of immunofluorescence (GFP, green; laminin, red; nuclei, blue; scale bar, 120 μm) and bioluminescence imaging (bioluminescence values are indicated as photons cm^{-2} $s^{-1} \times 10^5$; right).

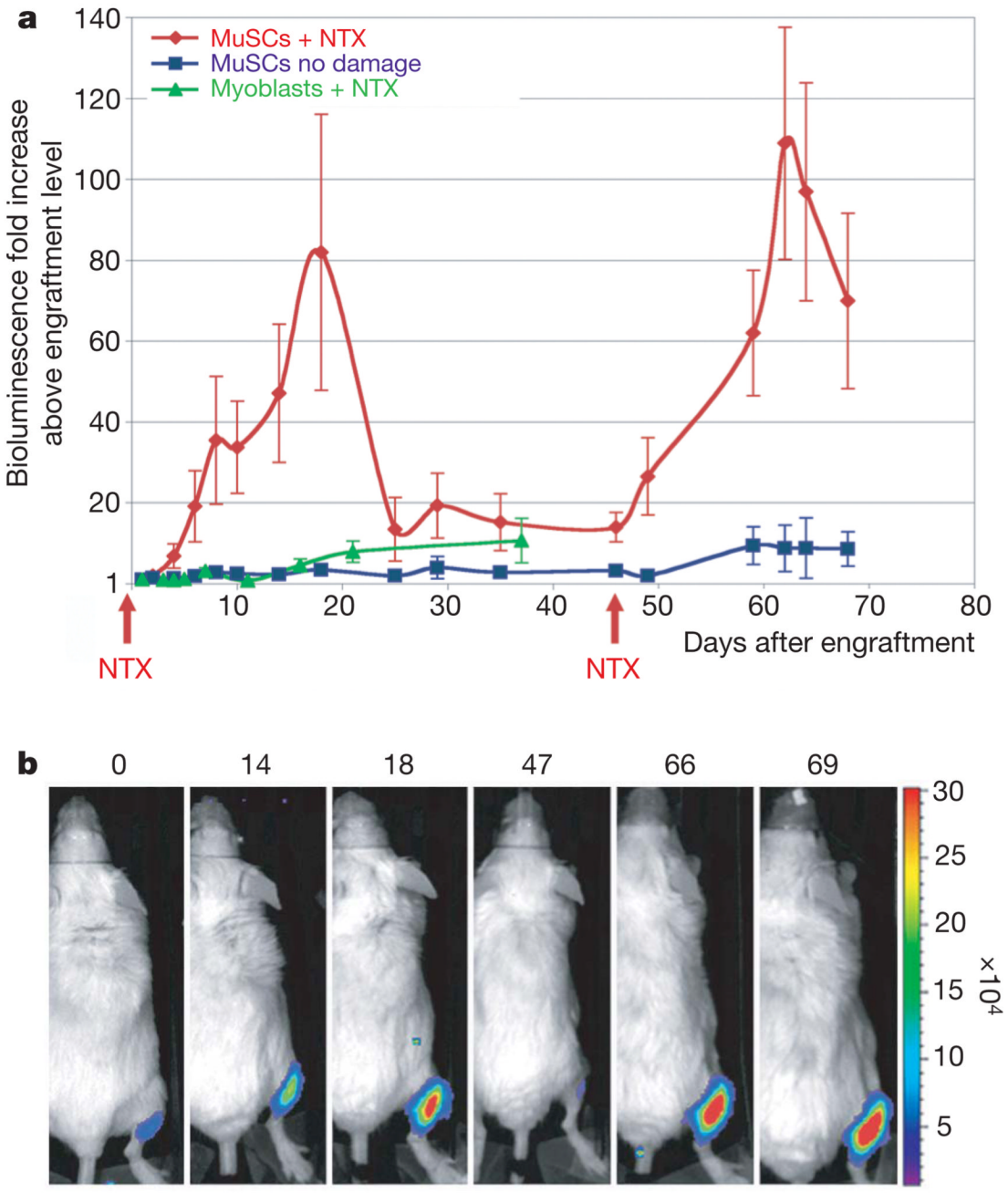

Figure 3. MuSC proliferation in response to muscle tissue damage

a, A low number of MuSCs (10–500) was transplanted into recipients (n = 10). After the engraftment plateau was reached (as in Fig. 2d), mice were divided into two groups, and the tibialis anterior muscles of one group were damaged by NTX injection, resulting in a substantial increase in cell numbers. At 47 days after the first damage, a second NTX injection led to a second increase in cell number, whereas no significant change was detected in the undamaged group. As a comparison, high numbers of primary myoblasts (4×10^5) were transplanted into recipients and four weeks later muscles were damaged by NTX injection. The average bioluminescence fold increase ± s.e.m. is shown (n = 5; $P < 0.05$). **b**, Bioluminescent images of a representative animal transplanted with MuSCs and damaged

with NTX acquired on the days indicated (top). Bioluminescence values are indicated as photons cm^{-2} s^{-1} × 10^4.

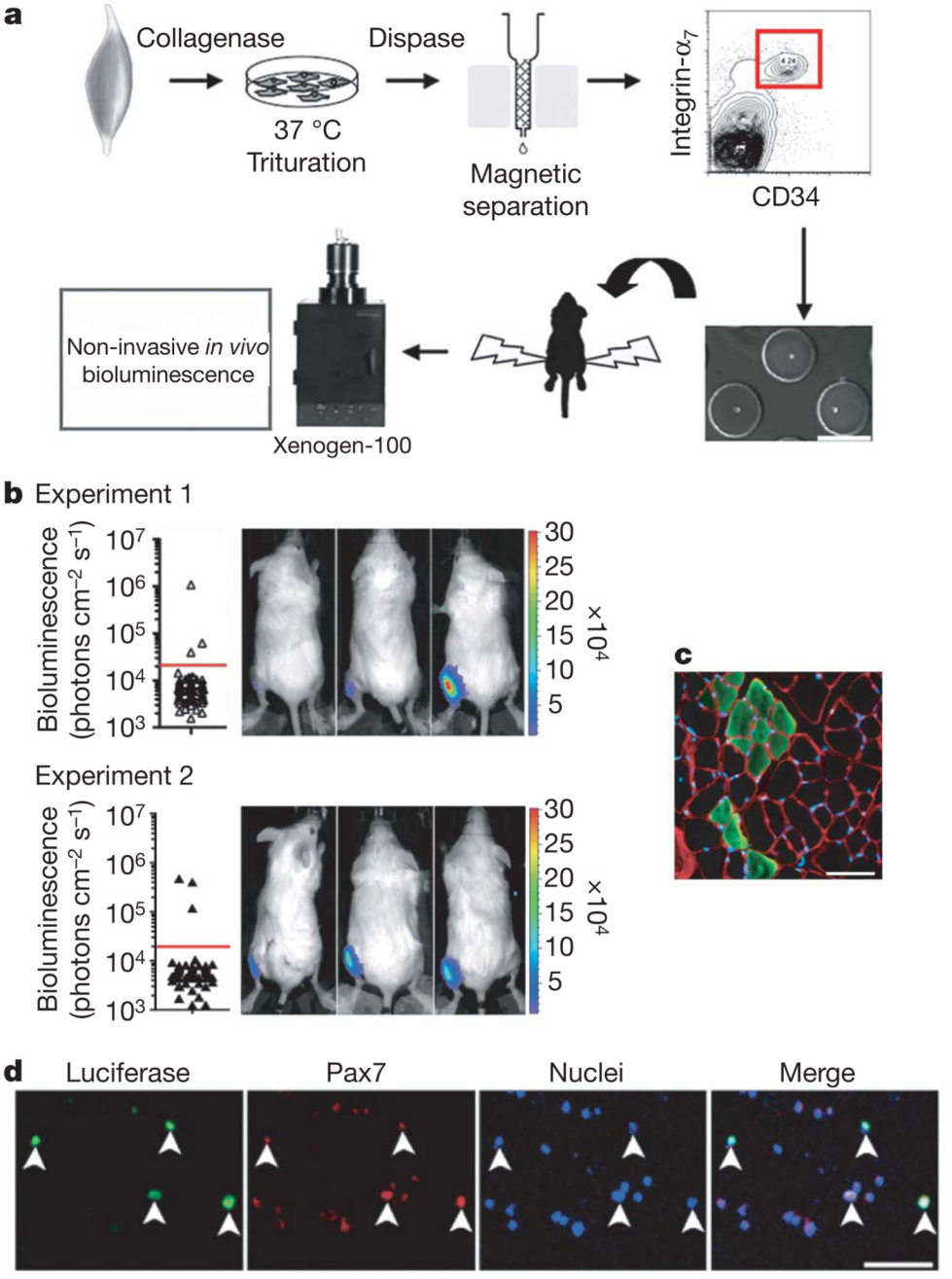

Figure 4. Transplantation of a single MuSC demonstrates self-renewal capacity

a, Scheme of single MuSC transplantation. Cells were isolated from *Myf5-nLacZ/FLuc* transgenic mice by FACS as in Fig. 1a, segregated as single cells in hydrogel microwells (< 10 µl per microwell; scale bars, 150 µm), individually picked by micromanipulation and transplanted into tibialis anterior muscles of recipient mice. **b**, Two independent experiments are shown (n= 6/144), and in each case 3 out of 72 single cell transplants resulted in engraftment above background detected by imaging mice four weeks after transplantation (left). Bioluminescent images of the 6 positive recipients after single MuSC transplantation (bioluminescence values are indicated as photons cm^{-2} s^{-1} × 10^4; right).

c, Immunofluorescence of luciferase expression in transverse muscle sections from the mice in **b** revealed the contribution of single MuSC progeny to muscle fibres. Laminin, red; luciferase, green; nuclei, blue. Scale bars, 50 μm. **d**, Muscle cells were re-isolated from mice transplanted with single cells, and donor-derived luciferase^{+}Pax7^{+} cells were detected. Scale bars, 100 μm.